

FRB-periodicity: mild pulsar in tight O/B-star binary

Maxim Lyutikov¹, Maxim Barkov^{1,2}, Dimitrios Giannios¹

¹ Department of Physics, Purdue University, 525 Northwestern Avenue, West Lafayette, IN 47907-2036, USA

² Astrophysical Big Bang Laboratory, RIKEN, 2-1 Hirosawa, Wako, Saitama 351-0198, Japan

ABSTRACT

The 16 days periodicity observed in the Fast Radio Burst (FRB) source FRB 180916.J0158+65 by the CHIME telescope is consistent with that of a tight, stellar mass binary system of semi-major axis \sim few $\times 10^{12}$ cm. The primary is an early OB-type star with mass loss rate $\dot{M} \sim 10^{-8} - 10^{-7} M_{\odot} \text{ yr}^{-1}$ and the secondary a neutron star. The observed periodicity is not intrinsic to the FRB's source, but is due to the orbital phase-dependent modulation of the absorption conditions in the massive star's wind. The observed relatively narrow FRB activity window implies that the primary's wind dynamically dominates that of the pulsar, $\eta = L_{sd}/(\dot{M}v_w c) \leq 1$, where L_{sd} is pulsar spin-down, \dot{M} is the primary's wind mass loss rate and v_w is its velocity. The condition $\eta \leq 1$ requires mildly powerful pulsar with $L_{sd} \lesssim 10^{37} \text{ erg s}^{-1}$. The observations are consistent with magnetically-powered radio emission originating in the magnetospheres of strongly magnetized neutron stars, the classical magnetars.

1. FRB periodicity due to the orbital motion with B-star companion

The CHIME collaboration announced a $P = 16$ day periodicity from FRB 180916.J0158+65 (The CHIME/FRB Collaboration et al. 2020). This is an important set of observations which sheds light on the origin of FRBs, as we discuss in the present Letter.

Let's first assume that the observed periodicity is due to the orbital motion of a binary system. The orbital semi-major axis then evaluates to

$$P = 2\pi \sqrt{\frac{a^3}{GM_{\odot}(m_{PSR} + m_{MS})}}$$

$$a = 4 \times 10^{12} m_{\text{tot},1}^{1/3} \text{ cm}, \quad (1)$$

where m_{PSR} is (the presumed) neutron star’s mass and m_{MS} is the primary’s mass (presumed to be a Main Sequence star) in Solar masses and $m_{\text{tot}} = (m_{PSR} + m_{MS})$. (We call the the O/B star “a primary”, while the neutron star ”companion”.) In this paper we use the notation $A_x = A/10^x$ and m_{tot} is measured in Solar masses M_{\odot} .

Both the pulsar, the *loci* of the FRB, and the primary produce winds: a relativistic wind by the pulsar and wind with velocity $v_w \sim \text{few } 10^3 \text{ km s}^{-1}$ by main-sequence star (Vink et al. 2001). We hypothesize that the observed periodicity is due to absorption of the FRB pulses in the primary’s wind, see Fig. 1.

The interacting pulsar’s and the primary’s winds create a conically shaped cavity around the less powerful source. The primary’s winds can be highly optically thick at radio waves due to free-free absorption, while the relativistic pulsar wind is, basically, transparent to radio waves. A transparent cone-like zone is, therefore, created behind the pulsar, modified into spiral structure by the orbital motion.

The radio waves propagating within this spiral structure do not experience free-free absorption. After they enter the primary’s wind, at larger distance, the wind’s density, and the corresponding absorption coefficient, are substantially reduced. Thus, the dynamics of interacting winds creates transparency windows when the observer sees the pulsar through the spiral structure (Bosch-Ramon & Barkov 2011; Bosch-Ramon et al. 2012, 2015).

Since the active window is observed to be less than 50% of the orbital period, *the primary’s wind should dominate over that of the pulsar*. This requires that the momentum parameter η is less than unity,

$$\eta = \frac{L_{sd}}{\dot{M}v_w c} \leq 1. \quad (2)$$

Furthermore, the typical opening of the transparency wedge behind a pulsar seen in simulations of Bosch-Ramon et al. (2015) is $\sim 15 - 20^\circ$; this is weakly dependent on the momentum parameter as long as $\eta \lesssim 0.3$. This is consistent with the active phase observed in FRB 180916.J0158+65.

The cavity created by the pulsar’s wind can reduce the absorption optical depth by a factor as large as 10^3 . Therefore, if at the location of the pulsar the primary’s wind is still moderately, $\tau \leq 10^3$, optically thick to infinity, and the observer’s line of sight lies close to the equatorial plane, within $\sim 15 - 20^\circ$, then the source turns transparent to radio emission for part of the orbit.

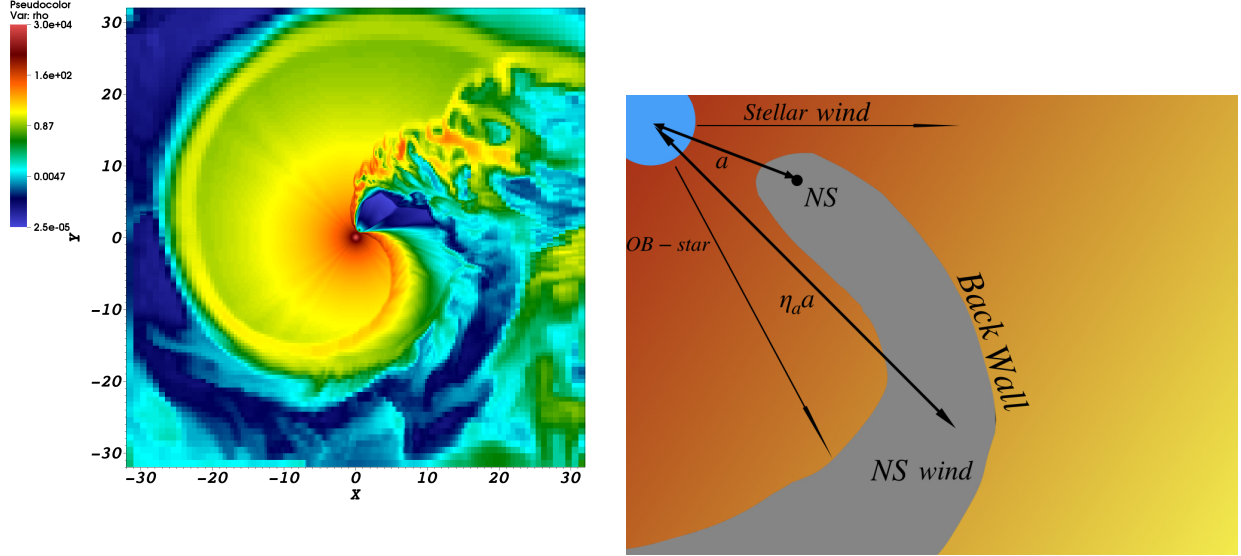


Fig. 1.— Left panel: reprocessed simulations of Bosch-Ramon et al. (2015) of interacting winds of B-star and pulsar’s. Right panel: artistic image of the interacting winds. The pulsar wind creates a narrow low density cavity that extends to distances much larger than the orbital separation by a factor $\eta_a \sim 10 - 30$. At that point the density of the companion’s wind is lower by η_a^2 , the absorption coefficient is reduced by η_a^4 , and optical depth by η_a^3 .

2. The model

Simulations of Bosch-Ramon et al. (2015), see also Fig. 1, demonstrate that the wind cavity can extend out to 10-30 times the binary separation radius. In the estimates below we parametrize the location of the “back wall” of the cavity as $\eta_a a$, and normalize the numerical estimates to $\eta_a = 10^{1.5} \eta_{a,1.5}$.

The free-free optical depth from the location of the “back wall” of the cavity to infinity should be of the order of unity for radio waves to escape. Using the free-free-absorption coefficient κ_{ff} (Lang 1999), assuming temperature $T = 10^4$ K, and scaling the “back wall” radius with the orbital separation (1), we find

$$\begin{aligned} \kappa_{ff} &= 3.28 \times 10^{-7} T_4^{-1.35} \nu_{1GHz}^{-2.1} \frac{EM}{pc} \\ \dot{M} &= 4\pi n m_p (\eta_a a)^2 v_w \\ \tau_{ff} &\sim 5 \times 10^{-3} \eta_{a,1.5}^{-3} \dot{M}_{-7.5}^2 T_4^{-1.35} \nu_{1GHz}^{-2.1} m_{tot,1} v_{w,8.5}^{-2}, \end{aligned} \quad (3)$$

here $EM = \int_a^\infty n^2 dr$ is emission measure. So, a mass loss rate of $\dot{M} \sim 3 \times 10^{-8} M_\odot/\text{yr}$

can give substantial optical depth to free-free absorption for a source at distance a but transparent conditions when the source is observed through the “back wall” of a cavity that extends to $\sim 30a$.

Using mass loss rate \dot{M} from (3) and requiring the primary’s momentum dominance in the wind-wind interaction, we estimate the pulsar spindown luminosity

$$L_{sd} \leq 5 \times 10^{36} \eta_{-0.5} \dot{M}_{-7.5} v_{w,8.5} \text{ erg s}^{-1}. \quad (4)$$

Thus, the pulsar can produce mildly strong winds.

The model limits the mass loss rate of the main sequence star both from below (the wind-wind interaction should be dominated by the Main Sequence star), and from above (too powerful winds are optically thick to free-free absorption out to very large distances). Early B-type stars, and late O-type stars fit the required mass loss range. Late B-type stars have insufficiently strong winds, while earlier O-type stars remain optically thick to large distances (Vink et al. 2001; Krtička 2014).

3. Nonlinear propagation effects

Strong radio waves can affect non-linearly the free-free absorption coefficient in the wind (Lu & Phinney 2019). Qualitatively, strong electromagnetic wave in weakly magnetized plasma induces electron’s oscillations with momentum

$$p_{\perp} \sim a_0 m_e c \\ a_0 = \frac{eE}{m_e c \omega}, \quad (5)$$

where a_0 is the laser intensity parameter, E is the electric field in the wave (Akhiezer et al. 1975). If the quiver energy $\sim a_0^2 m_e c^2$ is larger than temperature, $a_0 \geq \sqrt{T/(m_e c^2)}$, then the motion of the electrons is determined by the wave itself, not the temperature.

For typical parameters of FRB 180916.J0158+65 (The CHIME/FRB Collaboration et al. 2020) (total fluence $\mathcal{F} = 10$ Jy msec, duration $\tau = 2$ msec and distance $d_{FRB} = 150$ Mpc) the luminosity and the total energy in a single burst evaluate to

$$L_{FRB} = 4\pi \frac{d_{FRB}^2 \mathcal{F}}{\tau} = 3 \times 10^{40} \text{ erg s}^{-1}. \\ E_{FRB} = 4\pi d_{FRB}^2 \mathcal{F} = 6 \times 10^{37} \text{ erg}. \quad (6)$$

The nonlinearity parameter evaluates to

$$a_0 = \frac{e\sqrt{\mathcal{F}}}{am_e c^{3/2} \sqrt{\tau\omega}} \approx 1. \quad (7)$$

Thus, the FRB can heat the plasma to relativistic energies!

As the particles are heated by the wave, the plasma absorption coefficient κ_{ff} decreases, allowing a wave to propagate further. The total amount of the material the FRB heats is

$$M_h \sim \frac{m_p E_{FRB}}{a_0^2 m_e c^2} = 10^{20} \text{ g.} \quad (8)$$

This huge amount of material heated to relativistic electron temperatures is still much smaller than contained in the wind within the orbit

$$M_w \approx \frac{a}{v_w} \dot{M} = 3 \times 10^{22} \dot{M}_{-7.5} \text{ g} \quad (9)$$

or

$$\frac{M_h}{M_w} \approx 3 \times 10^{-3} \dot{M}_{-7.5}^{-1}. \quad (10)$$

Thus, a leading part of the FRB heats a part of the wind to relativistic energies, which makes it more transparent to the trailing part of the emission. But the FRB energetics is not sufficient to make the wind fully transparent, so the estimates in §2 remain valid. Also, the momentum implanted by the FRB pulse, $P_{FRB} \sim E_{FRB}/c \sim 2 \times 10^{27} \text{ g cm s}^{-1}$ is much smaller than the momentum of the wind within orbital radius, $P_w \approx a\dot{M} = 7 \times 10^{30} \dot{M}_{-7.5} \text{ g cm s}^{-1}$; the FRB pulse does not disturb the overall outflow. Moreover, the kinetic energy of the stellar wind $E_{w,kin} = M_w v_w^2/2 \approx 10^{39} \text{ ergs}$ is much larger compared to the FRB energy: $E_{FRB}/E_{w,kin} \sim 1/20$, so FRB impact on the flow dynamics can be neglected.

Non-linear effects are strongly suppressed by the magnetic field (Lyutikov 2019a, 2020). If the cyclotron frequency is larger than the wave frequency,

$$\omega_B \geq \omega \rightarrow B \geq 350\nu_9 \text{ G,} \quad (11)$$

then instead of large amplitude oscillations with p_\perp given by Eq. (5) a particles experiences E-cross-B drift. Magnetic fields of this order do occur in early type stars (*e.g.* Petit et al. 2019).

4. Unlikely alternative: FRB variations due to geodetic precession

Another possible source of variability is a the geodetic precession that make the active region periodically aligned with the line of sight. For example, in the binary pulsar PSR

0737 the geodetic precession lead to the disappearance of the PSR 0737B (Breton et al. 2008; Lomiashvili & Lyutikov 2014). To have a geodetic precession of only 16 days the required orbital size is

$$\Omega_G = \left(\frac{2\pi}{P} \right)^{5/3} \left(\frac{GM_\odot}{c^3} \right)^{5/3} \left(\frac{m_{MS}(4m_{PSR} + 3m_{MS})}{2(m_{PSR} + m_{MS})^{4/3}} \right)$$

$$a = 2 \times 10^9 \frac{(m_{MS}(4m_{PSR} + 3m_{MS}))^{2/5}}{(m_{PSR} + m_{MS})^{1/5}} \text{ cm} \quad (12)$$

Gravitational decay time is still sufficiently long,

$$t_{GW} = 670 \frac{m_{MS}^{2/5}}{m_{PSR}} \text{ yr} \quad (13)$$

(where $m_{MS} \geq m_{PSR}$ was assumed).

The system with separation of (12) will be exceptional. Strong modifications of the magnetospheric properties may be expected in this case. For example, setting separation equal to the light cylinder, the period would be 0.75 seconds. Strong wind-magnetosphere interactions are expected, similar to the case of the binary pulsar PSR0737A/B Lyutikov (2004); Lyutikov & Thompson (2005); Lomiashvili & Lyutikov (2014). Note, though, that PSR0737B is/was an *exceptionally weak pulsar* - it cannot not be used as an model for FRBs, the most powerful radio emitters.

Can still the radio emission be induced in FRB 180916.J0158+65 by the interactions of the companions? The orbital motionally-induced electric potential potential and luminosity for scaling (12) estimate to

$$\Phi_{orb} = eBa\beta_{orb} = 2 \times 10^{13} b_q \text{ eV}$$

$$L_{orb} \sim (\Phi_{orb}/e)^2 c = 2 \times 10^{31} b_q^2 \text{ erg s}^{-1}, \quad (14)$$

where we scaled the surface magnetic field to quantum field, $b_q = B_{NS}/B_Q$, $B_Q = m_e^2 c^3/(e\hbar)$.

Estimates (14) give very weak power, even for quantum-strong magnetic fields, and small potential. We conclude that even in the tightest orbit case of geodetically induced precession, the powers expected due to the interaction of the binaries are very small. *Hence we conclude that binarity is not a cause of FRB emission.*

5. Predictions

In this Section, we discuss the predictions of the model. As a simple educated guess, we predict variations of the dispersion measure within the observed window, and an increase of

the activity window at higher frequencies. First we give simple order-of-magnitude estimates, and then demonstrate that the reality is likely to be more complicated.

5.1. DM and optical depth variations: simple estimates

In a homogeneous wind a DM from a given point located distance a from the central star and propagating with angle ϕ

with respect to the radial direction (ϕ is assumed to be fixed - we neglect possible plasma lensing effects), is

$$DM(\phi) = \int_a^\infty \frac{n_0 a^2}{x^2 + (x - a)^2 \tan^2 \phi} \frac{dx}{\cos \phi} = \frac{\phi}{\sin \phi} DM_0, \quad (15)$$

where

$$DM_0 \approx 0.8 \dot{M}_{-7.5} \eta_{a,1.5}^{-1} m_{\text{tot},1}^{-1/3} v_{w,8.5}^{-1} \quad (16)$$

is the dispersion measure for a radial ray. (For larger ϕ the DM and the optical depth, see below, increase as the light ray passes longer distance at higher densities).

Similarly, in a homogeneous wind an optical depth to a given point (assuming isothermal wind) is

$$\begin{aligned} \tau(\phi) &\propto \int_a^\infty \left(\frac{n_0 a^2}{x^2 + (x - a)^2 \tan^2 \phi} \right)^2 \frac{dx}{\cos \phi} \\ \tau(\phi) &= \frac{3}{2} (\phi \csc^3(\phi) - \cot(\phi) \csc(\phi)) \tau_0 \end{aligned} \quad (17)$$

where $\tau_0 = \tau(\phi = 0)$ The optical depth for radial propagation depends on frequency, Eq. 3

$$\tau_0 \propto \nu^{-2.1} \quad (18)$$

Let ν_0 be the frequency such that $\tau_0(\nu_0 = 1)$. At higher frequencies optical depth of 1 is reached at angled pictured in Fig. 2.

5.2. DM and optical depth variations from numerical simulations

The above estimates assume idealized smooth wind. As numerical simulations demonstrate, Fig. 1, the plasma around the bow shock is highly inhomogeneous. The pulsar wind creates a tail cavity and an accumulation of dense material around the head. These plasma “wall” will have an especially large effect on the free-free absorption (see Fig.3), since it

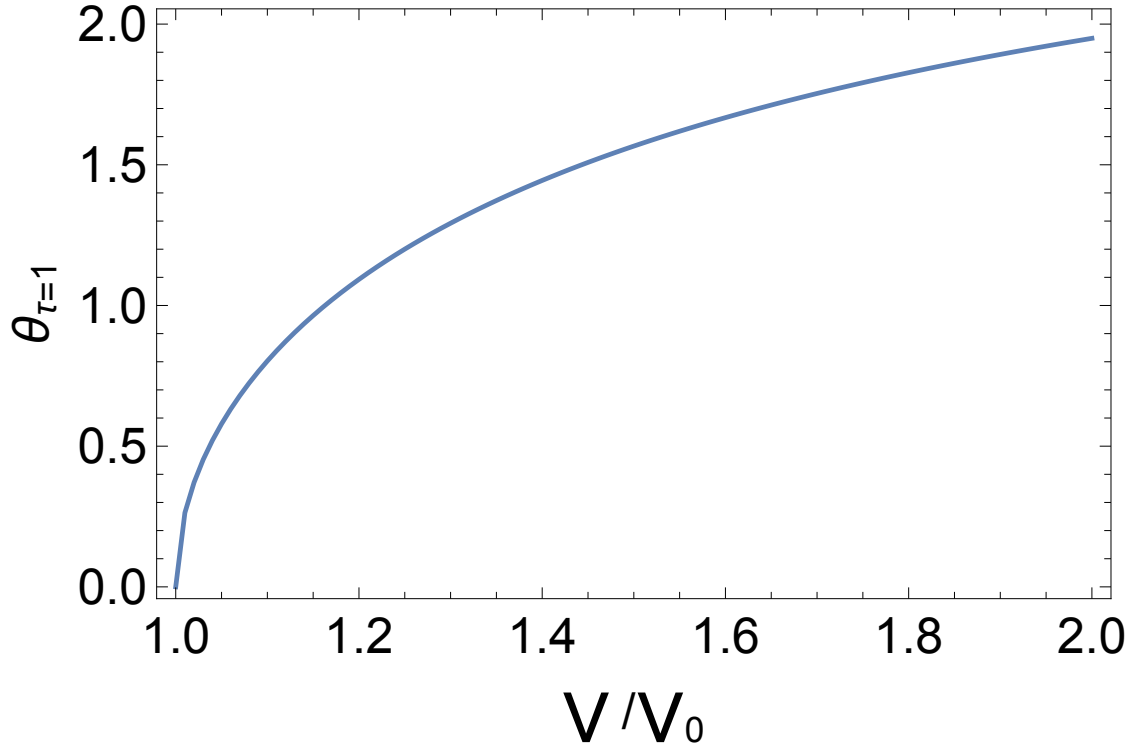


Fig. 2.— Dependence of the transparency angle ϕ on the observing frequency ν/ν_0 in idealized homogeneous wind. At the base frequency ν_0 the radial (outward propagating) rays have $\tau = 1$. At larger frequencies the rays at larger angles can escape, see also Fig. 4

depends on density squared. A plasma wall can be opaque to a broad range of frequencies, erasing a simple correlation between the active window and the observing frequency.

In the following, we calculate dispersion measure and free-free absorption using the 3-dimensional relativistic hydrodynamical simulation by Bosch-Ramon et al. (2015) who modeled the interaction of a massive stellar wind with the pulsar wind. In their setup, the pulsar is moving on elliptic orbit with eccentricity $e = 0.24$ and orbital period 3.4 days. For the following plots we reprocessed the data for the orbital period of 16 days. (Eccentricity for high mass binaries with compact object and orbital period about 15 days can vary from 0 till 0.85, Townsend et al. 2011; Tauris et al. 2017). In figure 4, we show the profiles of the integrated density, $\int n \propto DM$ and integrated density squared, $\int n^2 \propto \tau$ (the absorption optical depth) along different lines of sight. Fig. 4 demonstrates that at each moment there is a narrow transparency window with a duration from ~ 0.1 (close to apoastron) to ~ 0.3 (close to periastron) orbital period. Note that a wide transparency window can be affected by the turbulent motion and can be chaotically transparent and opaque from orbit to orbit.

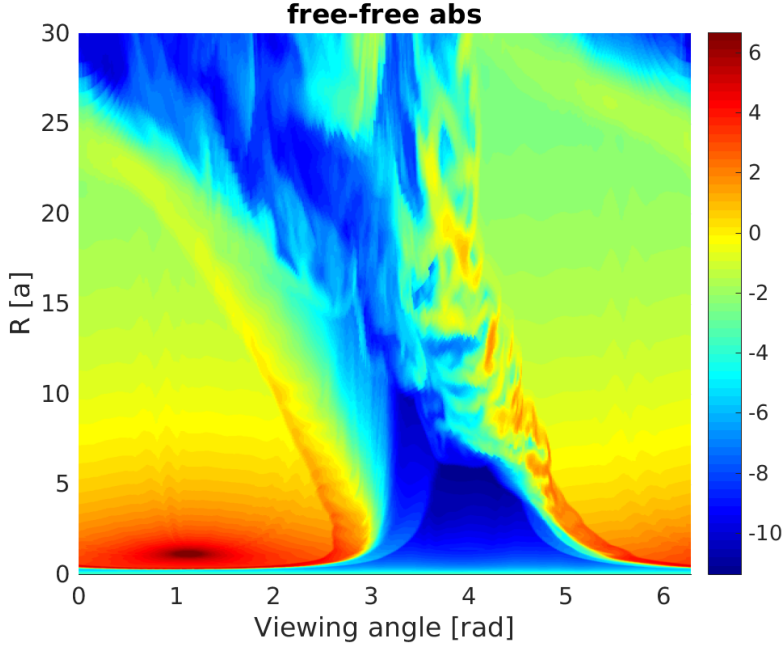


Fig. 3.— Profiles of the differential absorption optical depth (color) along different lines of sight calculated near apoastron orbital phase. Low values (blue color) corresponds to transparency window.

On the one hand, the DM and free-free absorption have a good correlation, the transparent window corresponds to a minimum of DM and it can explain the small change of DM for repeating FRBs. On the other hand, the variations of the DM within the transparency window are smaller by a factor of few than the overall variations.

6. Discussion

In this Letter we discuss a model for the periodicity observed in FRB 180916.J0158+65 by the CHIME telescope (The CHIME/FRB Collaboration et al. 2020). The working model is that the FRBs are produced by a neutron star that orbits an OB primary. The periodicity arises due to free-free absorption in the primary's (of the massive star's) wind. Thus, we argue that the observed periodicity is a property of a particular system and is likely not essential for the FRB production. On the other hand, the association of an FRB with a compact stellar binary further strengthens the magnetospheric *loci* of FRBs, as argued by (Popov & Postnov 2013; Lyutikov et al. 2016; Lyutikov 2019a,b) also (see reviews by

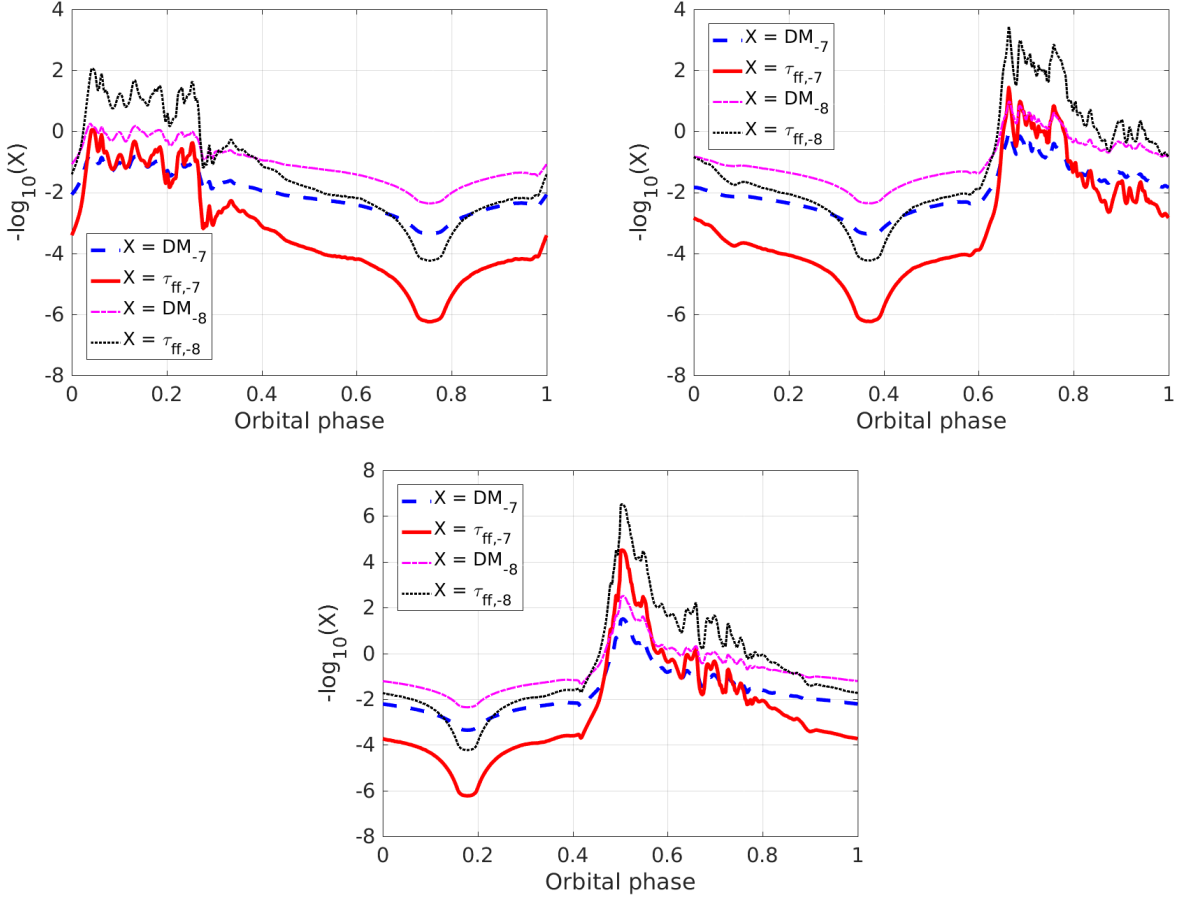


Fig. 4.— Profiles of the DM (dashed blue $\dot{M}_w = 10^{-7} M_\odot/\text{yr}$ and dot dashed magenta $\dot{M}_w = 10^{-8} M_\odot/\text{yr}$) and absorption optical depth (solid red $\dot{M}_w = 10^{-7} M_\odot/\text{yr}$ and dotted black $\dot{M}_w = 10^{-8} M_\odot/\text{yr}$) along different lines of sight calculated at three different orbital phases (close to apoastron - left, intermediate phase - center and close to periastron - right). Large values of $-\log \tau$ (red curves) correspond to transparency window.

Cordes & Chatterjee 2019; Petroff et al. 2019). Note that FRB 180916.J0158+65 also shows narrow emission bands drifting down in frequency - this is naturally interpreted as plasma laser operating in neutron star’s magnetosphere and showing radius-to-frequency mapping (Lyutikov 2019b).

Interestingly, a new, unusual radiative mechanism operates when an FRB pulse enters the companion’s wind: heating of a narrow layer of plasma to relativistic energies by a radio beam. We are not aware of such processes in any other astrophysical system. Corresponding bursts of X-ray emission are likely to be too weak to be observable.

We constrain the companion to be late O-type/early B-type star: earlier types have too powerful winds that remain heavily optically thick at the inferred orbital separation, while later types produce winds that are too weak - this runs contrary our interpretation of the small orbital activity window as a pointing to the momentum dominance of the primary's wind over the pulsar's. Since the primary's momentum loss should over-power the pulsar's wind - the pulsar can be only mildly strong, with a spin-down luminosity $L_{sd} \sim 10^{37}$ erg s $^{-1}$; this values is somewhat larger than the spin-down power of Galactic magnetars.

Periodic transparency can also be achieved by having a highly eccentric orbit - then at an apoastron the radio pulses would sample lower density plasma. We disfavor this scenario since it predicts a large active window (since the binary would spend more time at large separations).

Identification of FBRs with neutron stars leaves two possibilities for the energy source: rotational (akin to Crab's giant pulses Popov et al. 2006; Lyutikov 2007; Mickaliger et al. 2012; Lyutikov et al. 2016), or magnetar-like magnetically powered emission (Lyutikov 2002; Eichler et al. 2002).

To be clear, the term “magnetar” is used in two astrophysically separate settings: (i) powerful X-ray emitters, SRGs and AXPs, (eg Thompson & Duncan 1995; Thompson et al. 2002; Kaspi & Beloborodov 2017) ; (ii) fast pulsar with high magnetic field and high wind power (Usov 1992; Lyutikov 2006; Metzger et al. 2008). In the first case the radiative energy comes from the energy of the magnetic field in the latter case from the its rotational energy (strong magnetic field just serves to quickly transform the rotational energy into the wind). Many models of FRBs employ the second scenario, using the word “magnetar” to mean central source producing rotationally-powered winds (Margalit et al. 2019; Metzger et al. 2019; Beloborodov 2017). We argue that the present observations are inconsistent with the rotationally powered “fast-rotation pulsar with high magnetic field”-magnetar concept, but are consistent with magnetically-powered magnetospheric magnetar sources.

The present model has a number of similarities to binary systems containing pulsars. First, binary pulsars PSR 1957 + 20 and PSR 1744 - 24A shows periodic orbital-dependent eclipses (limited to $\sim 10\%$ in phase in case of PSR 1957 + 20 and $\sim 50\%$ in case of PSR 1744 - 24A Lyne et al. 1990; Rasio et al. 1989, 1991). These are mass binary, ablated by the NS's wind (Phinney et al. 1988), so the wind-wind interaction is dominated by the pulsar's wind, $\eta \geq 1$. In that case a number of plasma effects, like variations of the DM and pulse delays, do show during the eclipse. Then, there is a number of γ -ray binaries that contain (or thought to contain) neutron stars (Dubus 2013; Barkov & Bosch-Ramon 2016; Bosch-Ramon et al. 2017; Barkov & Bosch-Ramon 2018; Abeysekara et al. 2018)

Overall, the observed periodicity in FRB 180916.J0158+65 does fit with a general concept of neutron stars' magnetospheres being the *loci* of FRBs. It also confirms that FRBs are not rotationally powered (since the present model requires that the pulsar wind should be mild/weak). The magnetically powered model, radio emission generated in the magnetospheres of neutron stars remains the most probable, in our view.

Acknowledgments

ML would like to acknowledge support by NASA grant 80NSSC17K0757 and NSF grants 10001562 and 10001521. We would like to thank Victoria Kaspi, Jonathan Katz, Wenbin Lu and Elizaveta Ryspaeva for discussions and Yegor Lyutikov for help with the illustration.

REFERENCES

Abeysekara, A. U., et al. 2018, *ApJ*, 867, L19

Akhiezer, A. I., Akhiezer, I. A., Polovin, R. V., Sitenko, A. G., & Stepanov, K. N. 1975, Oxford Pergamon Press International Series on Natural Philosophy, 1

Barkov, M. V., & Bosch-Ramon, V. 2016, *MNRAS*, 456, L64

—. 2018, *MNRAS*, 479, 1320

Beloborodov, A. M. 2017, *ApJ*, 843, L26

Bosch-Ramon, V., & Barkov, M. V. 2011, *A&A*, 535, A20

Bosch-Ramon, V., Barkov, M. V., Khangulyan, D., & Perucho, M. 2012, *A&A*, 544, A59

Bosch-Ramon, V., Barkov, M. V., Mignone, A., & Bordas, P. 2017, *MNRAS*, 471, L150

Bosch-Ramon, V., Barkov, M. V., & Perucho, M. 2015, *A&A*, 577, A89

Breton, R. P., et al. 2008, *Science*, 321, 104

Cordes, J. M., & Chatterjee, S. 2019, *ARA&A*, 57, 417

Dubus, G. 2013, *A&A Rev.*, 21, 64

Eichler, D., Gedalin, M., & Lyubarsky, Y. 2002, *ApJ*, 578, L121

Kaspi, V. M., & Beloborodov, A. M. 2017, *ARA&A*, 55, 261

Krtička, J. 2014, *A&A*, 564, A70

Lang, K. R. 1999, *Astrophysical formulae*

Lomiashvili, D., & Lyutikov, M. 2014, *MNRAS*, 441, 690

Lu, W., & Phinney, E. S. 2019, arXiv e-prints, arXiv:1912.12241

Lyne, A. G., et al. 1990, *Nature*, 347, 650

Lyutikov, M. 2002, *ApJ*, 580, L65

—. 2004, *MNRAS*, 353, 1095

—. 2006, *New Journal of Physics*, 8, 119

—. 2007, *MNRAS*, 381, 1190

—. 2019a, arXiv e-prints, arXiv:1901.03260

—. 2019b, arXiv e-prints, arXiv:1909.10409

—. 2020, arXiv e-prints, arXiv:2001.09210

Lyutikov, M., Burzawa, L., & Popov, S. B. 2016, *MNRAS*, 462, 941

Lyutikov, M., & Thompson, C. 2005, *ApJ*, 634, 1223

Margalit, B., Berger, E., & Metzger, B. D. 2019, *ApJ*, 886, 110

Metzger, B. D., Margalit, B., & Sironi, L. 2019, *MNRAS*, 485, 4091

Metzger, B. D., Quataert, E., & Thompson, T. A. 2008, *MNRAS*, 385, 1455

Mickaliger, M. B., et al. 2012, *ApJ*, 760, 64

Petit, V., et al. 2019, *MNRAS*, 489, 5669

Petroff, E., Hessels, J. W. T., & Lorimer, D. R. 2019, *A&A Rev.*, 27, 4

Phinney, E. S., Evans, C. R., Blandford, R. D., & Kulkarni, S. R. 1988, *Nature*, 333, 832

Popov, M. V., Soglasnov, V. A., Kondrat'Ev, V. I., Kostyuk, S. V., Ilyasov, Y. P., & Oreshko, V. V. 2006, *Astronomy Reports*, 50, 55

Popov, S. B., & Postnov, K. A. 2013, arXiv e-prints, arXiv:1307.4924

Rasio, F. A., Shapiro, S. L., & Teukolsky, S. A. 1989, *ApJ*, 342, 934

—. 1991, *A&A*, 241, L25

Tauris, T. M., et al. 2017, *ApJ*, 846, 170

The CHIME/FRB Collaboration et al. 2020, arXiv e-prints, arXiv:2001.10275

Thompson, C., & Duncan, R. C. 1995, *MNRAS*, 275, 255

Thompson, C., Lyutikov, M., & Kulkarni, S. R. 2002, *ApJ*, 574, 332

Townsend, L. J., Coe, M. J., Corbet, R. H. D., & Hill, A. B. 2011, *MNRAS*, 416, 1556

Usov, V. V. 1992, *Nature*, 357, 472

Vink, J. S., de Koter, A., & Lamers, H. J. G. L. M. 2001, *A&A*, 369, 574